

8-1-2018

Imaging the Surface of a Hand-Colored 19th Century Daguerreotype.

Madalena S Kozachuk

Maria O Avilés

Ronald R Martin

Brianne Potts

Tsun-Kong Sham

See next page for additional authors

Follow this and additional works at: <https://ir.lib.uwo.ca/chempub>

 Part of the [Chemistry Commons](#)

Citation of this paper:

Kozachuk, Madalena S; Avilés, Maria O; Martin, Ronald R; Potts, Brianne; Sham, Tsun-Kong; and Lagugné-Labarthe, François, "Imaging the Surface of a Hand-Colored 19th Century Daguerreotype." (2018).

Chemistry Publications. 209.

<https://ir.lib.uwo.ca/chempub/209>

Authors

Madalena S Kozachuk, Maria O Avilés, Ronald R Martin, Brianne Potts, Tsun-Kong Sham, and François Lagugné-Labarthe

Submitted paper

Imaging the surface of a hand coloured Nineteenth century daguerreotype

Madalena S. Kozachuk, Maria O. Avilés, Ronald. R. Martin, Brianne Potts, Tsun-Kong Sham, François Lagugné-Labarthet*

The University of Western Ontario (Western University), Department of Chemistry, 1151 Richmond Street, London, Ontario, N6A 5B7, Canada

Abstract

Daguerreotypes are valued artifacts that constitute a unique historical photographic memory of the 19th century. Understanding their surface chemistry is important in order to conserve and, when necessary, to restore them. Coloured highlights were often added by hand to emphasize different features on the daguerreotype's subjects. In the present work we report on a daguerreotype that was hand coloured with a red pigment that was added to the cheeks of the two subjects. A series of experiments using micro-Raman and micro-FTIR spectroscopy and synchrotron-based X-ray fluorescence microscopy and absorption spectroscopy are used to analyze the surface and to determine the nature of the pigment used as well as the common elements present in the fabrication of the daguerreotypes.

Key Words

Daguerreotypes, Pigments, Raman spectroscopy, FTIR spectroscopy, synchrotron X-ray fluorescence microscopy, scanning electron microscopy, pigments.

Corresponding Author:

François Lagugné-Labarthet, The University of Western Ontario, The Department of Chemistry, 1151 Richmond Street, London, Ontario, N6A 5B7, Canada

Email: flagugne@uwo.ca

Introduction

The development of the first commercially viable photographic process, the daguerreotype, supplied the first permanent photochemical method of historical preservation. Known for their stunning resolution and wide range of grey tones, daguerreotypes captured portraits and landscapes for a span of approximately 25 years between 1839 and 1860. Daguerre's original process starts with a highly polished, silver-coated copper plate that was sensitized to visible light through the exposure to iodine vapour. Successive developments of the sensitization process included further exposures to bromine and chlorine, which increased the sensitivity of the silver plate and drastically reduced the exposure time of the plates. Exposure to light catalyzes the formation of silver image particles that produce a latent image on the photosensitive plate, which is then fixed with heated mercury vapour. Residual silver halide is removed with a sodium thiosulfate solution, rendering the developed plate insensitive to light. The gilding step was later added by Fizeau where the treatment of the daguerreotype with a gold chloride solution increases the contrast and improves the durability of the final image.¹⁻³

While Louis-Jacques-Mandé Daguerre's original process² and other subsequent improvements⁴ produced brilliant 19th century representations, the commercial demand for coloured images lead to the addition of pigments over these delicate surfaces. Due to long exposure times in the original process, daguerreotypes often showed softened tones or blurred portions of the image as well as expressionless faces of the living subjects.⁵ Colouring was often added to mask these defects and other production flaws, as well as for artistic reasons such as highlighting details.⁶ Given the popular interest in producing photographs at the end of the 19th century, including albumen prints,⁷ the processes used in daguerreotype production were widely reported in literature.^{6, 8-10} The work from Willat⁸ notes that the most common colouring pigments used on daguerreotypes were carmine, rouge, chrome yellow, burnt sienna, ultramarine and white and that they should be "stippled on (not rubbed) with a small camel's-hair brush". Often, dry pigment powders were mixed with gum Arabic (also finely powdered), linseed oil or applied with a varnish onto of the completed daguerreotype.¹¹ Simons' publication on different photographic methods noted when colouring daguerreotypes, carmine or pink madder are appropriate for tinting the cheek regions of portraits.¹² It should be expected however, that the colouring of daguerreotypes was not limited to these pigments, as daguerreotypists would have utilized whatever was available and cost-effective for their practice.

Little attention has been paid to the examination of hand-coloured daguerreotypes although the chemical composition, origin, and degradation of pigments is of considerable interest in the scientific museum community.¹³⁻²⁰ Of the little work that has been completed on identifying pigments on hand-coloured 19th century plates, blues have been attributed to Prussian blue ($\text{Fe}_4[\text{Fe}_3(\text{CN})_6] \cdot n\text{H}_2\text{O}$) and rouge tones have been attributed to Mars red (Fe_2O_3).^{11, 21}

The objectives of this study were i) to determine the composition of a red pigment present on a hand-coloured daguerreotype. Scanning electron microscopy combined with dispersive X-ray spectroscopy (SEM-EDX) was used to determine the morphology of the pigment particles and to estimate the elemental composition of the pigments and the surface. Raman and Fourier transform infrared microspectroscopies were used to identify the red pigment crystals found on the cheeks of the subjects and evaluate if binders were used; ii) to determine the presence of other inorganic compounds on the daguerreotype using synchrotron based X-ray absorption near edge structure (XANES) spectroscopy and X-ray fluorescence (XRF) microscopy. The combination of XANES spectra and XRF mapping allowed one to measure the distribution of iron oxide particles presumably used in the polishing of the daguerreotype as well as other elements such as chlorine and sulfur.

Materials and Methods

Sample

The 19th century daguerreotype examined in this study was purchased from an antique bookstore (Attic Book, London, ON, Canada) (**Figure 1**). At the time of purchase, the daguerreotype was in a frame including a cover glass. Upon removal of the plate from its case, text was found within the interior frame, which supplied the title of the image, *Bust of Lady*, the family name of the two subjects (Rounds) and the location of origin (Wood River, Nebraska, USA). Presumably developed in the mid-19th century, this historic daguerreotype was acquired by Attic Books from the estate of Don Hensley, a former professor in English studies department at The University of Western Ontario, London, ON.



Figure 1. (a) Photograph of the studied daguerreotype after removal of the encapsulating frame. (b) Backside of frame that contained identification of family name and location.

Reference Dye Sample

Carminic acid (Alum lake of carminic acid) was purchased from Fischer Scientific and was used as the reference sample. CAS: 1390-65-4 Purity Grade: Pure Assay: $\geq 42.0\%$ (carminic acid).

Scanning Electron Microscopy

Scanning electron microscopy images were collected with a LEO (Zeiss) 1540XB FIB/SEM equipped with a EDX detector (Oxford Instruments X max 50 detector). Energy dispersive X-ray spectroscopy examination was collected with the SEM EDX detector and analysis was performed with INCA analysis software. Imaging was performed at 1 kV with a working distance of 4 mm and backscattered imaging at 10 kV and 9 mm. The intensity of the collected X-rays were used to quantify the carbon K α -edge, oxygen K α -edge, sulfur K α -edge, silver L α -edge, gold M α -edge, and mercury M α -edge.

Fourier Transform Infrared Spectroscopy

Fourier transform infrared spectra were collected using a Thermo Scientific Nicolet Continuum FTIR Microscope under reflectance mode, with a liquid nitrogen-cooled mercury cadmium telluride detector, x15/0.58 NA objective and a resolution of 2 cm⁻¹. The number of scans ranged between 128 and 200.

Raman Spectroscopy

Raman spectra were recorded with a LabRAM HR (Horiba Scientific) spectrometer combined with a confocal microscope using an excitation wavelength of 785 nm. A liquid nitrogen-cooled CCD detector with a 600 grooves/mm grating and a pinhole set at 150 μm pinhole were used. A microscope objective of x100/0.9 NA was used. Acquisition times varied between 10 to 40 s. At the sample, the laser power was recorded at 500 μW for the 785 nm laser for the daguerreotype and 5 mW for reference powder pigments. All measurements were collected in the backscattering geometry.

Synchrotron Radiation Analysis

Two-dimensional XRF maps and the XANES spectra were collected at the SXRMB (06B1-1) line of the Canadian Light Source (CLS) using the medium energy X-ray microprobe end station.²² An incident energy of 7130 eV, just above the Fe K-edge of 7112 eV, was utilized for the XRF mapping. Elements of interest for the XRF maps were Ag, Au, Hg, Cl, I, Si, S, and Fe. A 4-element Si(Li) drift detector set with a CCD camera was used and the sample was mounted on a 3-axis (X, Y and Z) sample stage. A micro-ion chamber was

placed in between the Kirkpatrick-Baez (KB) micro-focusing mirrors for beam alignment and monitoring. The spot size of the beam at the specimen was $\sim 10 \mu\text{m} \times 10 \mu\text{m}$. X-ray fluorescence maps were created and analyzed using the SMAK software program.²³ All XRF maps were normalized to I_0 . The beam was monochromatized by a Si(111) double crystal monochromator; Ag, Cl, and S XANES were collected in fluorescence (FLY) mode by setting an energy window at the Ag $L\alpha$ and the Cl and S $K\alpha$ fluorescence. The Ag L_3 -edge XANES was collected with a 2.00 eV step size below, 0.15 eV step size at, and 0.75 eV step size above the edge. The Cl K-edge XANES was collected with the same set of parameters. The S K-edge was collected with a 2.00 eV steps below, 0.20 eV step at, and a 0.75 eV step above the edge. Calibration, background subtraction, normalization, and averaging of all collected spectra were conducted using the Athena software package.²⁴ The inflection point at the edge was determined by taking the first derivative of each spectrum following the procedure outlined by Ravel.²⁵

Results and Discussion

Microscopy Examination and Elemental Distribution with SEM-EDX

The daguerreotype image is formed as a result of the reflection and scattering of light by the image particles on the surface. These image particles, which vary in size, shape, and distribution depending on the relative light intensity received during the exposure, produce a range of grey tones that characterize the daguerreian image.^{26, 27} Regions exposed to a relatively greater light intensity (i.e., highlight regions; **Figure 2a**) produced image particles relatively uniform in structure and density (defined as the number of image particles per unit area). For highlight areas the particle density has been estimated as $\sim 2 \times 10^5$ particles/mm². Little to no exposure (i.e., dark regions; **Figure 2b**) yielded image particles variable in size and shape with low surface density (< 100 particles/mm²). These particle density values only serve as relative estimates and not absolute figures, for differing production environments (i.e., intensity of light, time of exposure, nature of the silver halide layer, etc.) will impact the image particle density on the daguerreotype surface. Examples of daguerreotype particles distribution are shown in **Figure 2** from three distinct areas. The woman's left eye was chosen for analysis as it contains both dark and light areas. This particle distribution is consistent with previous work.⁴ The SEM images collected of the cheek region (**Figure 2c**) shows that there are a variety of pigment particles present, with many of them appearing as octahedral-shaped crystals with dimensions less than $1 \mu\text{m}$ and organized as aggregates. The pigment particles are surrounded by image particles that are evenly dispersed and relatively uniform in size and shape, consistent with those observed in highlight regions.

The density of the image particles on the cheek is lower than that observed in the white of the woman's left eye thus producing a less white region as

compared to the eye. Relative to the image particles in the eye region, the ones on the cheek do appear to be flattened. This may be due to the method in which the pigment was possibly applied using a small brush.⁸

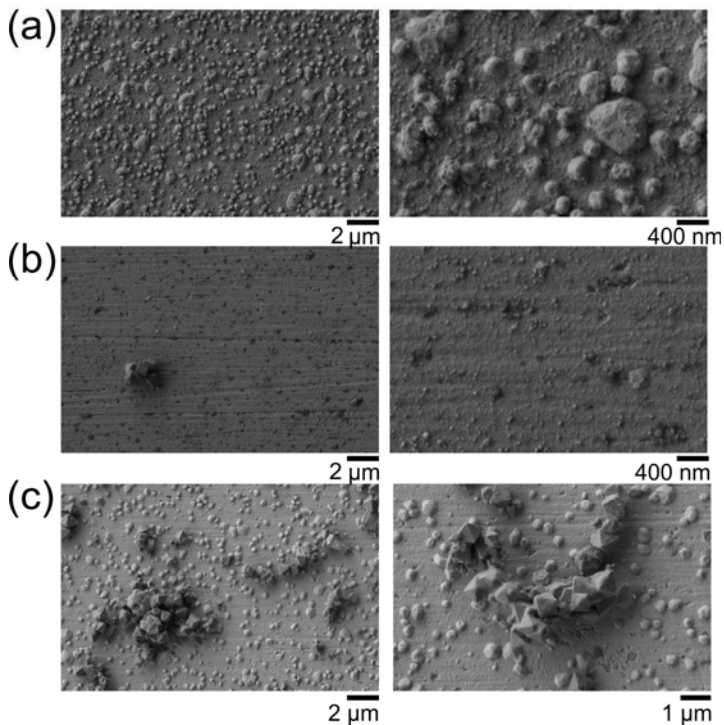
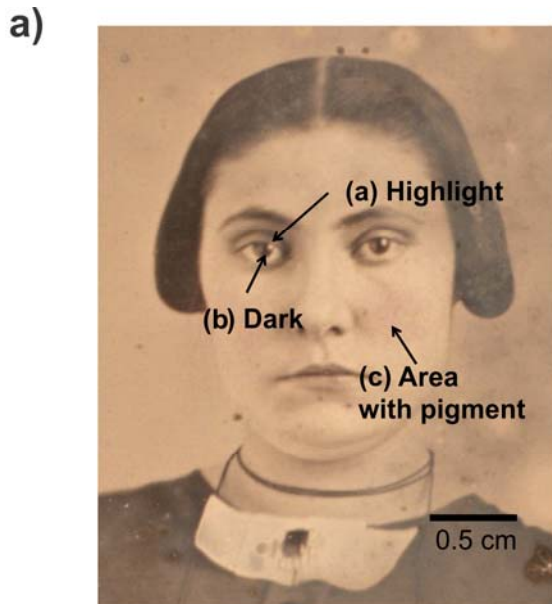


Figure 2. Secondary electron SEM imaging of (a) highlight, (b) dark, and (c) coloured regions from the *Bust of Lady* daguerreotype. (a) Highlight region collected from the white of woman's left eye with (b) dark region collected from the woman's left iris. (c) Coloured region collected from the woman's left cheek.

Energy dispersive X-ray spectroscopy combined with the SEM instrument, was used to study the distribution of C, O, Fe, Ag, S and Hg in the vicinity of pigments as shown in **Figures 3a-h**. The distribution of O and C are co-localized with the pigment meanwhile the silver distribution is the weakest on the location of the pigment due to a shadowing effect from the pigment. In these specific locations (**Figures 3b,c**), the atomic % was determined for both C and O. Weight percentage of 26.2% was measured for C and 20.33 weight % for O. Presence of Al is confirmed (0.48% weight) and is also co-localized with the pigment crystals (**Figure 3d**) due to the presence of Al center in the dye structure. Although only the pigment particles were selected to determine the elemental weight percentages, a strong contribution of Ag substrate is present in these measurements (42.8% weight, **Figure 3e**) emphasizing the limitation of using EDX to determine quantitatively the composition of the pigment particle alone. Other elements such as Au (6.31% weight), Cu (1.63% weight) were detected as well as traces of Na (0.31% weight), Mg (0.28% weight), S (0.27% weight, **Figure 3f**), Ca (0.67% weight) and Hg (0.42% weight, **Figure 3g**) were detected. Interestingly the presence of Au indicates that the daguerreotype was gilded to increase its contrast.

While Fe was observed with SEM-EDX the iron particles appear to be distributed evenly over the surface of the daguerreotype (**Figure 3h**) and do not appear to be constituent of an iron-based pigment such as Mars red.^{10, 21} The presence of iron particles is presumably originating from the polishing agent used to attain the mirror finish, which required for a high quality image in the production process.²⁸ Additionally, **Figures 3f,g** show the distribution of S and Hg, which are contained in the particles forming the image particles and appear to be co-localized. These particles are forming the optical contrast in the Daguerre photography process.⁴

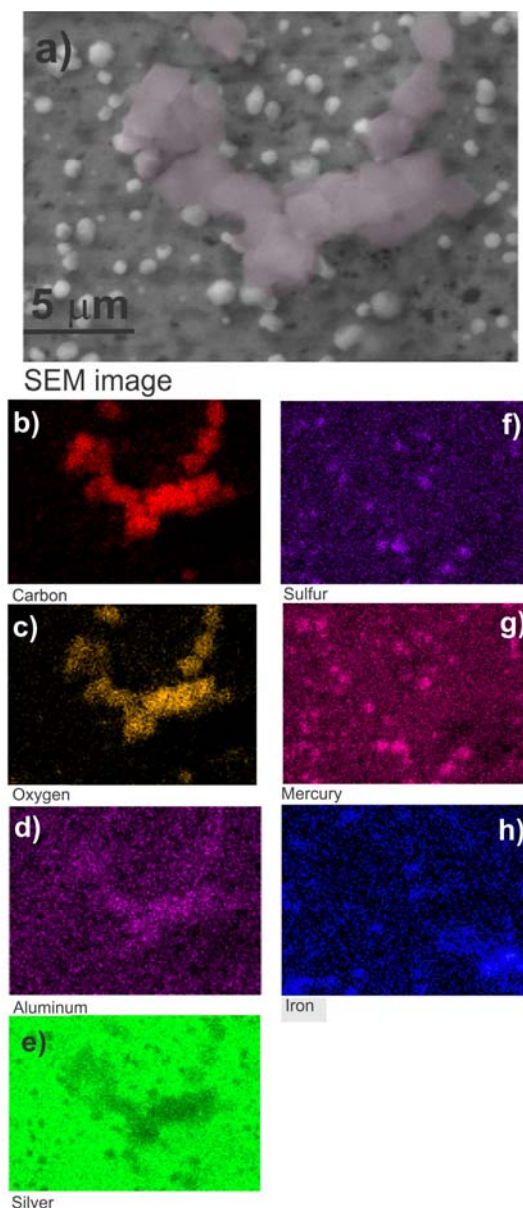


Figure 3. (a) An SEM image of the selected area. The elemental distribution for C (b), O (c) and Al (d) match the morphology of the dye crystals shown in (a). The distribution of silver (e) shows an inverted contrast with a weaker silver signal in the regions corresponding to the dye crystals. Other elements like S (f), Hg (g) and Fe (h) are distributed randomly over the silver surface. The pigment crystals of the SEM image in (a) have been slightly colorized for better visualization.

RAMAN Analysis

Raman microscopy measurements were conducted on pigment particles that could be localized under an optical microscope. Aggregates of red pigments

could be easily observed using 100x N.A. 0.9 microscope objective. The excitation laser at 785 nm was selected because of reduced fluorescence background inherent to probing colourful dyes. A variety of red pigments, which were used in mid-19th century art production for pigments as well as binders, were examined as references using Raman and FTIR microscopy. The spectra of alizarin crimson, alizarin, carminic acid were also collected but did not show any common spectral features with the pigments present on the daguerreotype. Shown in **Figure 4** are the Raman spectra of pure carmine and the pigment used to colour the daguerreotype shown in **Figure 2c**. The matching of the two spectra clearly lead to the identification of the carmine pigment as the material used to colour the cheeks of the subjects. The spectra acquired on the daguerreotype were much more sensitive to the laser power than for the pure pigment. SERS effects from the underlying silver substrate were possibly the source of a more highly localized electromagnetic field, which might result in photo-induced damage. For this reason the excitation intensity of the laser source was limited to 500 μ W for the daguerreotype sample.

The wavenumbers associated with the Raman spectra of the carmine dye and the crystals present on daguerreotype were compared and are reported in Table I. The 1100-1660 cm^{-1} region is characteristic of the carmine pigment^{29, 30} and matches the red pigment spectra on the daguerreotype as shown in **Figure 4a**. Specifically, the main peaks observed in the daguerreotype were located at 1103, 1253, 1310, 1414, 1479, 1530 cm^{-1} . The 1103 cm^{-1} (m) and the 1310 cm^{-1} (s) bands can be assigned to the C-C stretching.³¹ The contributions at 1184, 1414, 1479 and 1530 cm^{-1} with medium intensities correspond to bending (C-H) bond, stretching (C=C-O⁻), stretching (C=C)+bending (C-H), and stretching (COO⁻), respectively.^{29, 32-34} Finally there is a very weak wavenumber band of 1655 cm^{-1} , which corresponds to a stretching (C=O) or (C=C).³² Furthermore, the weak band at 858 cm^{-1} is related to the Al-OH and is indicative of the carmine aluminum complex.³⁵ In addition, there is another band (1300-1320 cm^{-1}) corresponding to a stretching COO⁻ that is also bonded to the aluminum complex. That was noticed in previous studies when comparing carminic acid pigment spectra, not having aluminum centered complex, to carmine pigment.^{36, 37}

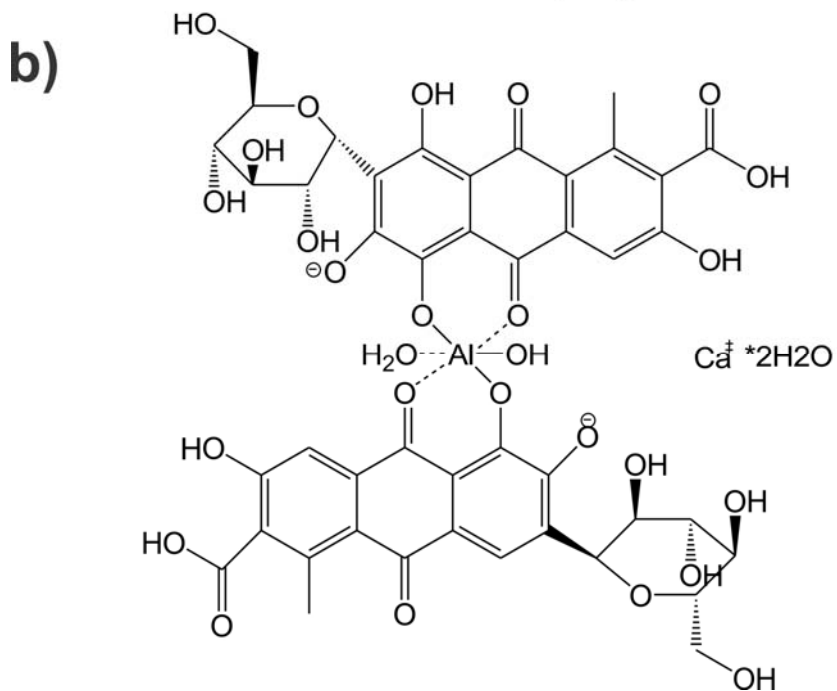
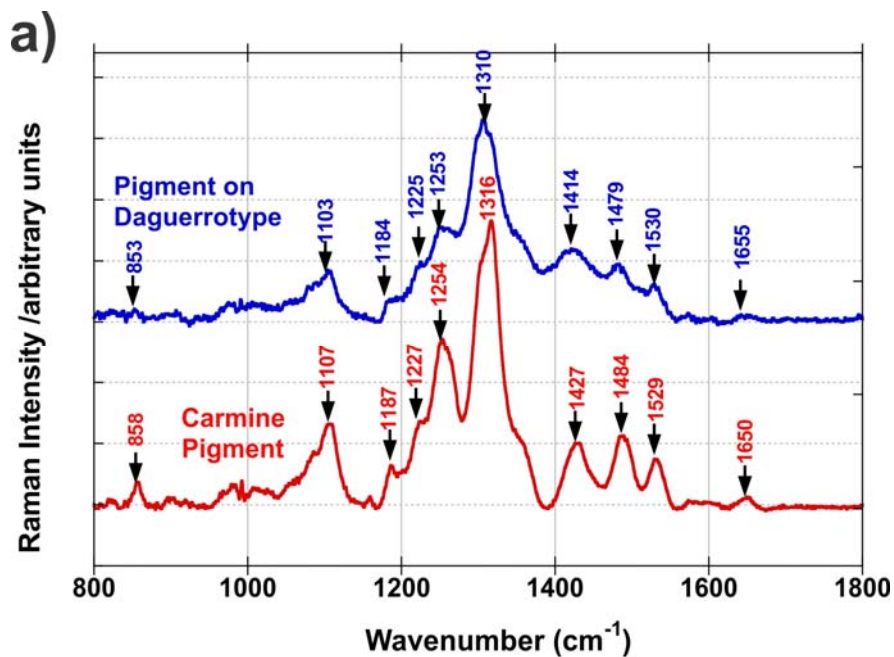


Figure 4. (a) Raman spectra of pigments located on the cheeks of the two subjects and reference Raman spectra acquired on pure carmine pigment. (b) Molecular structure of carmine.

Table I. Wavenumbers of the carmine and dye crystals on daguerreotype and assignment of the vibrational modes. ν , stretching; δ , bending. vs: very strong, s: strong, m: medium, w: weak, vw: very weak.

Carmine reference Wavenumber (cm⁻¹)	Daguerreotype Wavenumber (cm⁻¹)	Assignment
858w	853vw	$\nu(\text{Al-OH})$
1107m	1103m	$\delta(\text{C-C})$
1187w	1184m	$\delta(\text{C-H})$
1227w	1225w	$\nu(\text{CH}_2)+\nu(\text{C-H})$
1254s	1253m	$\nu(\text{C=C}), \delta(\text{C-OH}), \delta(\text{C-H})$
1316vs	1310s	$\delta(\text{C-OH}), \nu(\text{C-C})$
1426m	1414m	$\nu(\text{C=C-O}^-)$
1484m	1479m	$\nu(\text{C=C})+\delta(\text{C-H})$
1529m	1530m	$\nu(\text{COO}^-)$
1650w	1655vw	$\nu(\text{C=O})+\nu(\text{C=C})$

FTIR Analysis

Micro-FTIR mapping measurements were conducted on the daguerreotype surface as well as carmine reference deposited on a polished silver plate. The resulting spectra are shown in **Figure 5**. The spectra show similarities but the relative contributions of the overlapping bands in the [1000-1800] cm⁻¹ spectral range are not necessarily identical. These differences may arise from the properties of the supporting silver surfaces, different metals used in the preparation of carmine from carminic acid and/or the degradation in the environment.³⁸ The daguerreotype silver has obviously undergone a variety of chemical exposures and may have been subject to varying environments over the past 150 years. In contrast, the reference pigment was deposited over a freshly prepared and polished silver surface. The background reflectance spectra were conducted for each sample (i.e. the daguerreotype and the polished silver) on a selected area on the silver plate without the presence of particles. The difference of background may also explain the spectral differences observed in the FTIR spectra. However, despite these differences, these FTIR spectra are in substantial agreement with the Raman spectra and support the use of carmine for the colouring of the daguerreotype. The IR spectra were compared against binders such as Arabic gum and linseed oil excluding their presence in the present coloured daguerreotype.

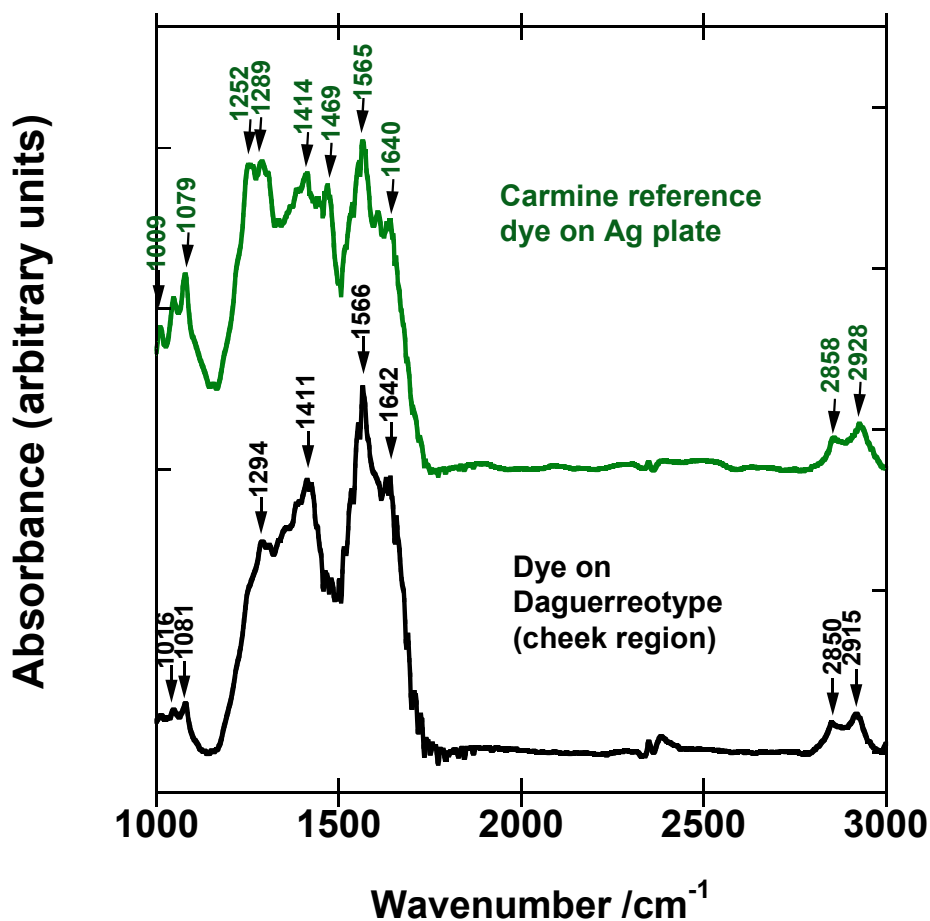


Figure 5. Micro-FTIR spectra collected on the reference carmine dye deposited as powder onto a freshly polished silver plate and pigment deposited approximately 150 years ago onto a daguerreotype plate.

Table II. FTIR spectra of carmine pigment and crystals on the daguerreotype. ν : stretching, δ : bending. vs: very strong, s: strong, m: medium, w: weak, vw: very weak, sh: sharp.

Carmine pigment Wavenumber (cm^{-1})	Daguerreotype Wavenumber (cm^{-1})	Assignment
1009m,sh ; 1079s; 1252m; 1289m	1016w, 1081w, 1294w	$\delta(\text{C-O})$
1414m	1411s	$\delta(\text{O-H})$
1469m	---	$\delta(\text{C-H})$
1565s,sh	1566s, sh	$\nu(\text{C=C})$ aromatic
1640w	1642w	$\nu(\text{C=C})$
2858w, 2928w	2850w, 2915w	$\nu(\text{C-H})$

The main IR bands found on the daguerreotype are located at 1016, 1081, 1294, 1411, 1566, 1642, 2850 and 2915 cm^{-1} and are summarized in Table II. The functional groups associated to the indicated bands coincide with the chemical structure of carmine. Bending and stretching (C-O) modes are observed for the 1016, 1081 and 1294 cm^{-1} peaks that may be due to the presence of glucose. In particular the band at 1081 cm^{-1} is assigned to the scissoring mode of glucose (C-O) and (O-H).³⁹ The medium peak of 1411 cm^{-1} indicates a bending (O-H) that correspond to a carboxylic acid.⁴⁰ The aromatic rings contained in the carmine structure have characteristic strong and weak bands located at 1566 and 1642 cm^{-1} , respectively. The bands of 2858 and 2928 cm^{-1} , both defined as weak peaks, correspond to a stretching (C-H)³⁹.

Synchrotron SXRF and XANES Analysis

X-ray fluorescence imaging and XANES spectroscopy analysis of the woman's left cheek is shown in

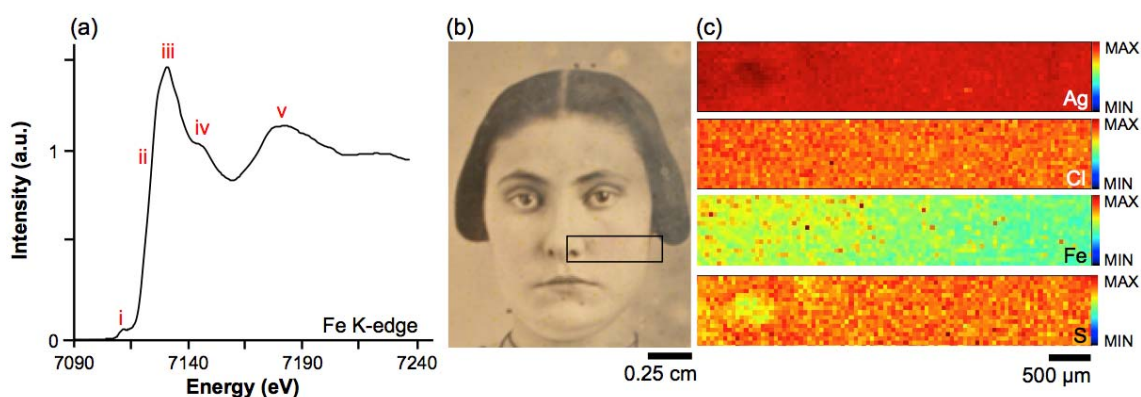


Figure 6. The distribution of iron in the XRF image in **Figure 6** is identical to that obtained by SEM-EDX (**Figure 3**). This dissemination is consistent with the use of an iron-based abrasive during preparation of the silver plate rather than the result post-production pigmentation.

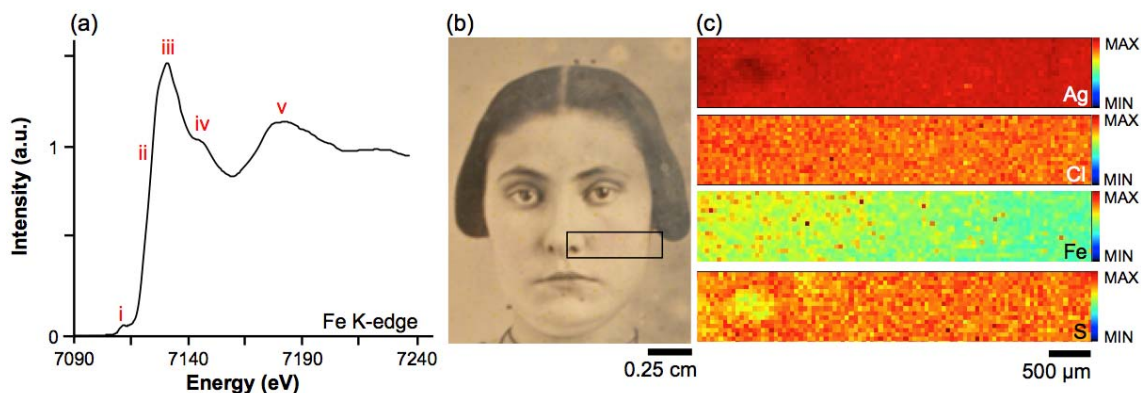


Figure 6. (a) XANES spectra for Fe collected from the woman's cheek. The location of the spot analyzed is by a circle on the synchrotron XRF Fe image. (b) Selected area on the woman's face for the synchrotron XRF image collection. (c) Synchrotron XRF images collected from the woman's left cheek. Only Ag, Cl, Fe and S are shown for clarity.

Three primary features make up the iron K-edge: a weak pre-edge feature (i = 7110 eV) that is the result of a formally dipole-forbidden transition, a shoulder (ii = 7123.2 eV) on the absorption edge from a $1s \rightarrow 4s$ transition (iii = 7130 eV), and a $1s \rightarrow 3d$ transition after the edge (iv = 7141.8 eV).⁴¹ These features are followed by a broad oscillation at 7183.4 eV (peak v). As the location of the absorption threshold is indicative of the Fe–O bond length (i.e. a shorter interatomic distance corresponds to a higher edge location)⁴² the XANES technique is extremely sensitive to the chemical environment and local geometry of the element of interest. The location of the edge jump as well as the location of the oscillations within the XANES spectrum, which was collected in the vicinity of a coloured region on the woman's left cheek, shows the presence of both γ - Fe_2O_3 and α - Fe_3O_4 , indicative of a mixture of Fe^{2+} and Fe^{3+} present on the surface. This finding, along with the distribution pattern observed in the XRF image and EDX elemental mapping is consistent with the use of an iron oxide polishing agent during preparation of the silver plate.

Figure 7 shows the XRF maps for Ag, Cl, S, and Fe collected from the woman's left eye away from any dye crystals. This region was chosen for its wide range of gray tones within a small region. The variable intensity of the Ag fluorescence image may be attributed to X-ray absorption by gold and mercury in the image particles. The sulfur distribution shows a close association with the image particles and may be the result of the thiosulfate used in fixing the image, during gilding, and/or trace atmospheric gases.^{4, 27, 43, 44} The chlorine may be residual silver chloride, residue from the gilding step and/or trace atmospheric gases.²⁷ Silver chloride, which is one of the most commonly identified tarnishes on daguerreotype surfaces, could also arise from post-production conditions. For instance, typical concentrations of chlorine within the museum environment has been reported as HCl (0.4 ppb).^{45, 46} The distribution of iron shows a uniform pattern across the selected eye area, which also matches the distribution signal

from the cheek region, an observation consistent with the use of an iron-based abrasive during daguerreotype production.

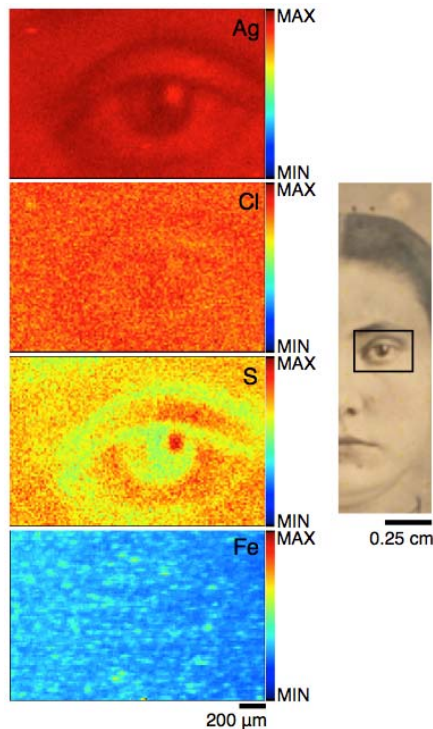


Figure 7. XRF maps of Ag, Cl, S, and Fe from the woman's left eye region.

Conclusions

Examination of pigment on the daguerreotype surface is challenging due to the complexity of the surface as well as low concentrations of the pigment. Fe K-edge XANES revealed iron oxide present on the surface. While iron oxide was used in the hand-colouring of 19th century daguerreotypes, the distribution observed in the Fe XRF maps collected at both the eye and cheek of the woman are consistent with residue from the polishing agent. The SEM-EDX results are supporting this finding since Fe was not associated with the pigment particles. Fourier transform infrared spectroscopy and Raman spectra obtained from the coloured area are essentially identical to those obtained from a carmine reference sample. The identification of carmine, an organic pigment, on the surface of this daguerreotype suggests that any conservation procedures applied to coloured areas should avoid exposure of these regions to solvents likely to dissolve organics. Submersion in cleaning solvent may be detrimental to the integrity of the original image unless preliminary tests of carmine pigment on a silver substrate demonstrate to be resistant to the proposed cleaning methods. Future work will address these limitations inherent to these hand-coloured plates.

Funding

This research was supported by the National Science and Engineering Research Council of Canada, the Canadian Foundation for Innovation, Canada Research Chairs (TKS, FLL) and the Ontario Ministry of Innovation. MSK wish to thank the support of the Canadian Photography Institute at the National Gallery of Canada. Further support for interdisciplinary research was provided by The Dean's Office at The University of Western Ontario, Faculty of Science. The authors wish to acknowledge Todd Simpson at the Western Nanofabrication facility for SEM and EDX imaging. Synchrotron experiments were performed at the Canadian Light Source, which is supported by NSERC, NRC, CIHR and the University of Saskatchewan.

References

1. P. Ravines, L. Li, L. Chan, R. McElroy. "Some Science Behind the Daguerreotype: Nanometer and Sub-micrometer Realities On and Beneath the Surface", In: P. Dillman, L. Bellot-Gurlet and I. Nenner, Eds. *Nanoscience and Cultural Heritage*, Paris: Atlantis Press, 2016.
2. E. Da Silva, M. Robinson, C. Evans, A. Pejović-Milić, D. V. Heyd, "Monitoring the Photographic Process, Degradation and Restoration of 21st Century Daguerreotypes by Wavelength-Dispersive X-Ray Fluorescence Spectrometry". *J. Anal. At. Spectrom.*, 2010. 25(5): 654-661.
3. M. S. Kozachuk, R. R. Martin, T. K. Sham, M. Robinson, A. J. Nelson, "The Application of XANES for the Examination of Silver, Gold, Mercury, and Sulfur on the Daguerreotype Surface". *Can. J. Chem.*, 2017. 95(11): 1156-1162.
4. P. Ravines, L. Li, R. McElroy, "An Electron Microscopy Study of the Image Making Process of the Daguerreotype, the 19th Century's First Commercially Viable Photographic Process". *J. Imaging Sci. Techn.*, 2016. 60(3): 10.
5. M. Robinson. *The Techniques and Material Aesthetics of the Daguerreotype*. [PhD Thesis]. Leicester, England: De Montfort University, 2017.
6. S. D. Humphrey. *American Hand Book of the Daguerreotype: Giving the Most Approved and Convenient Methods for Preparing the Chemicals, and the Combinations Used in the Art. Containing the Daguerreotype, Electrotype, and Various Other Processes Employed in Taking Heliographic Impressions*. New York: S. D. Humphrey, 1853.
7. C. Ricci, S. Bloxham, S. G. Kazarian, "ATR-FTIR Imaging of Albumen Photographic Prints". *J. Cult. Herit.*, 2007. 8(4): 387-395.
8. J. H. Croucher. *Willats's Scientific Manuals, No. 1. Plain Directions for Obtaining Photographic Pictures by the Calotype and Energiatype and other Processes on Paper; Including Chrysotype, Cyanotype, Chromotype, etc., etc., with all the latest improvements*. London: T. & R. Willats, 1844.
9. A. Bisbee. *The History and Practice of Daguerreotyping*. New York: Arno Press, 1973.
10. M. A. Gaudin. "A General Review of the Daguerreotype", In: H. H. Snelling, Ed. *The Photographic Art-Journal*, New York: Smith W.B., 1853. 5, 354-358.
11. D. Anglos, K. Melesanaki, V. Zafirooulos, M. J. Gresalfi, J. C. Miller, "Laser-Induced Breakdown Spectroscopy for the Analysis of 150-Year-Old Daguerreotypes". *Appl. Spectrosc.*, 2002. 56(4): 423-432.
12. M. P. Simons. *Photography in a Nut Shell; Or, The Experience of an Artist in Photography, on Paper, Glass and Silver, With Illustrations*. Philadelphia: King & Baird, 1858.
13. L. M. Smieska, R. Mullett, L. Ferri, A. R. Woll, "Trace Elements in Natural Azurite Pigments Found in Illuminated Manuscript Leaves Investigated by Synchrotron X-Ray Fluorescence and Diffraction Mapping". *Appl. Phys. A*, 2017. 123: 484.
14. L. Burgio, R. J. Clark, T. Stratoudaki, M. Doulgeridis, D. Anglos, "Pigment Identification in Painted Artworks: A Dual Analytical Approach Employing Laser-

- Induced Breakdown Spectroscopy and Raman Microscopy". *Appl. Spectrosc.*, 2000. 54(4): 463-469.
15. I. Reiche, K. Müller, M. Albéric, O. Scharf, A. Wähning, A. Bjeoumikhov, M. Radtke, R. Simon, "Discovering Vanished Paints and Naturally Formed Gold Nanoparticles on 2800 Years Old Phoenician Ivories Using SR-FF-MicroXRF with the Color X-ray Camera". *Anal. Chem.*, 2013. 85(12): 5857-5866.
 16. F. Vanmeert, G. Van der Snickt, K. Janssens, "Plumbonacrite Identified by X-ray Powder Diffraction Tomography as a Missing Link During Degradation of Red Lead in a Van Gogh Painting". *Angew. Chem. Int. Edit.*, 2015. 127(12): 3678-3681.
 17. D. C. Creagh, "The Characterization of Artefacts of Cultural Heritage Significance Using Physical Techniques". *Radiat. Phys. Chem.*, 2005. 74(6): 426-442.
 18. K. Melessanaki, V. Papadakis, C. Balas, D. Anglos, "Laser Induced Breakdown Spectroscopy and Hyper-Spectral Imaging Analysis of Pigments on an Illuminated Manuscript". *Spectrochim. Acta B*, 2001. 56(12): 2337-2346.
 19. B. Hochleitner, V. Desnica, M. Mantler, M. Schreiner, "Historical Pigments: a Collection Analyzed with X-Ray Diffraction Analysis and X-Ray Fluorescence Analysis in Order to Create a Database". *Spectrochim. Acta B*, 2003. 58(4): 641-649.
 20. A. Derbyshire, R. Withnall, "Pigment Analysis of Portrait Miniatures Using Raman Microscopy". *J. Raman Spectrosc.*, 1999. 30(3): 185-188.
 21. L. Grinde. Conservation of Stereo Daguerreotype: Examination and Documentation of the Characteristics. [Advanced Residency Program in Photograph Conservation, 3rd Cycle]. Rochester: George Eastman House International Museum and Image Performance Institute, 2005.
 22. Y. F. Hu, I. Coulthard, D. Chevrier, G. Wright, R. Igarashi, A. Sitnikov, B. W. Yates, E. L. Hallin, T. K. Sham, R. Reininger, "Preliminary Commissioning and Performance of the Soft X-ray Micro-characterization Beamline at the Canadian Light Source", in The 10th International Conference on Radiation Instrumentation, Melbourne (Australia), Sept 27–Oct 2, 2009. R. Garrett, I. Gentle, K. Nugent and S. Wilkins, Eds. *AIP Conf. Proc.* 2010. 1234(1): 343-346.
 23. S. M. Webb, "The MicroAnalysis Toolkit: X-ray fluorescence image processing software", in The 10th International Conference on X-ray Microscopy, Chicago, Illinois, (USA), Aug 15-20, 2010. I. McNulty, C. Eyberger and B. Lai, Eds. *AIP Conf. Proc.* 2011. 1365(1): 196-199.
 24. B. Ravel, M. Newville, "ATHENA, ARTEMIS, HEPHAESTUS: Data Analysis for X-Ray Absorption Spectroscopy Using IFEFFIT". *J. Synchrotron Radiat.*, 2005. 12(4): 537-541.
 25. B. Ravel. "ATHENA user's guide". 2009.
<http://bruceravel.github.io/demeter/documents/Athena/index.html> [accessed February 21st 2017]
 26. I. Motoyoshi, S. Nishida, L. Sharan, E. H. Adelson, "Image Statistics and the Perception of Surface Qualities". *Nature*, 2007. 447(7141): 206-209.

27. S. M. Barger, W. B. White. *The Daguerreotype: Nineteenth-Century Technology and Modern Science*. Washington D.C: Smithsonian Institution Press, 1991.
28. W. Watts. "Polishing Powder", In: W. Watts, Ed. *A Dictionary of Chemistry and the Allied Branches of Other Sciences*, London, UK: Longmans, Green and Co., 1877. 4, 686.
29. E. Svobodová, Z. Bosáková, M. Ohlídalová, M. Novotná, I. Němec, "The Use of Infrared and Raman Microspectroscopy for Identification of Selected Red Organic Dyes in Model Colour Layers of Works of Art". *Vib. Spectrosc.*, 2012. 63: 380-389.
30. Y. X. Wu, P. Liang, Q. M. Dong, Y. Bai, Z. Yu, J. Huang, Y. Zhong, Y. C. Dai, D. Ni, H. B. Shu, C. U. Pittman, "Design of a Silver Nanoparticle for Sensitive Surface Enhanced Raman Spectroscopy Detection of Carmine Dye". *Food Chem.*, 2017. 237: 974-980.
31. F. S. Manciu, L. Reza, L. A. Polette, B. Torres, R. R. Chianelli, "Raman and Infrared Studies of Synthetic Maya Pigments as a Function of Heating time and Dye concentration". *J. Raman Spectrosc.*, 2007. 38(9): 1193-1198.
32. N. Peica, I. Pavel, S. Cîntă Pînzaru, V. K. Rastogi, W. Kiefer, "Vibrational Characterization of E102 Food Additive by Raman and Surface-Enhanced Raman Spectroscopy and Theoretical Studies". *J. Raman Spectrosc.*, 2005. 36(6-7): 657-666.
33. N. Peica, W. Kiefer, "Characterization of Indigo Carmine with Surface-Enhanced Resonance Raman Spectroscopy (SERRS) Using Silver Colloids and Island Films, and Theoretical Calculations". *J. Raman Spectrosc.*, 2008. 39(1): 47-60.
34. N. D. Bernardino, D. L. A. de Faria, A. C. V. Negrón, "Applications of Raman Spectroscopy in Archaeometry: An Investigation of Pre-Columbian Peruvian Textiles". *J. Archaeol. Sci. Rep.*, 2015. 4: 23-31.
35. A. Guedes, B. Valentim, A. C. Prieto, A. Sanz, D. Flores, F. Noronha, "Characterization of Fly Ash from a Power Plant and Surroundings by Micro-Raman Spectroscopy". *Int. J. Coal Geol.*, 2008. 73(3): 359-370.
36. S. Liu, A. Odate, I. Buscarino, J. Chou, K. Frommer, M. Miller, A. Scorese, M. C. Buzzeo, R. N. Austin, "An Advanced Spectroscopy Lab that Integrates Art, Commerce, and Science as Students Determine the Electronic Structure of the Common Pigment Carminic Acid". *J. Chem. Educ.*, 2017. 94(2): 216-220.
37. R. W. Dapson, "The History, Chemistry and Modes of Action of Carmine and Related Dyes". *Biotech. Histochem.*, 2007. 82(4-5): 173-187.
38. L. M. R. Bowers, S. J. S. Sobek, "Impact of Medium and Ambient Environment on the Photodegradation of Carmine in Solution and Paints". *Dyes Pigments*, 2016. 127: 18-24.
39. M. C. Rosu, R. C. Suci, M. Mihet, I. Bratu, "Physical-Chemical Characterization of Titanium Dioxide Layers Sensitized with the Natural Dyes Carmine and Morin". *Mat. Sci. Semicon. Proc.*, 2013. 16(6): 1551-1557.
40. J. Van der Weerd, R. M. A. Heeren, J. J. Boon, "Preparation Methods and Accessories for the Infrared Spectroscopic Analysis of Multi-Layer Paint Films". *Stud. Conserv.*, 2004. 49(3): 193-210.

41. A. N. Maratkanova, A. V. Syugaev, D. A. Petrov, S. F. Lomayeva, "Structural Characterization and Microwave Properties of Chemically Functionalized Iron Particles Obtained by High-Energy Ball Milling in Paraffin-Containing Organic Environment". *Powder Technol.*, 2015. 274: 349-361.
42. C. Piquer, M. A. Laguna-Marco, A. G. Roca, R. Boada, C. Guglieri, J. Chaboy, "Fe K-Edge X-Ray Absorption Spectroscopy Study of Nanosized Nominal Magnetite". *J. Phys. Chem. C*, 2014. 118(2): 1332-1346.
43. T. E. Graedel, D. T. Hawkins, L. D. Claxton. *Atmospheric Chemical Compounds: Sources, Occurrence and Bioassay*. Orlando: Academic Press, 1986.
44. J. E. Yocom, W. L. Clink, W. A. Cote, "Indoor-Outdoor Air Quality Relationships". *Air Pollut. Contr. Assoc.*, 1971. 21(5): 251-259.
45. S. Hackney, "The Distribution of Gaseous Air Pollution Within Museums". *Stud. Conserv.*, 1984. 29(3): 105-116.
46. M. W. M. Hisham, D. Grosjean, "Sulfur Dioxide, Hydrogen Sulfide, Total Reduced Sulfur, Chlorinated Hydrocarbons and Photochemical Oxidants in Southern California Museums". *Atmos. Environ. A-Gen.*, 1991. 25(8): 1497-1505.